Synthesis, Structural Characterization, and Olefin Polymerization Behavior of Vanadium(III) Complexes Bearing Bidentate Phenoxy-Phosphine Ligands

Sen-Wang Zhang,[1,2] Ling-Pan Lu,[1,2] Bai-Xiang Li,[1] Yue-Sheng Li[1]

[1]State Key Laboratory of Polymer Physics and Chemistry, Changchun Institute of Applied Chemistry, Chinese Academy of Sciences, Changchun 130022, China
[2]Graduate School of the Chinese Academy of Sciences, Changchun Branch, Changchun 130022, China
Correspondence to: Y.-S. Li (E-mail: ysli@ciac.jl.cn)

Received 12 June 2012; accepted 26 July 2012; published online
DOI: 10.1002/pola.26292

ABSTRACT: Vanadium(III) complexes bearing phenoxy-phosphine ligands (**2a–g**) (2-R_1-4-R_2-6-PPh_2-C_6H_2O)$VCl_2(THF)_2$ (**2a**: $R_1 = R_2 = H$; **2b**: $R_1 = F$, $R_2 = H$; **2c**: $R_1 = Ph$, $R_2 = H$; **2d**: $R_1 = t$Bu, $R_2 = H$; **2e**: $R_1 = R_2 = Me$; **2f**: $R_1 = R_2 = t$Bu; **2g**: $R_1 = R_2 = CMe_2Ph$) were prepared from $VCl_3(THF)_3$ by treating with 1.0 equiv of the ligand in tetrahydrofuran (THF) in the presence of excess triethylamine (TEA). The reaction of $VCl_3(THF)_3$ with 2.0 equiv of the ligand in THF in the presence of excess TEA afforded vanadium(III) complexes bearing two phenoxy-phosphine ligands (**3c–f**). These complexes were characterized by FTIR and mass spectrum as well as elemental analyses. Structures of **2f** and **3c** were further confirmed by X-ray crystallographic analyses. Complexes **2a–g** and **3c–f** were employed as the catalysts for ethylene polymerization under various reaction conditions. On activation with Et_2AlCl, these complexes exhibited high catalytic activities (up to 41.3 kg PE/mmol$_V$·h·bar) even at high temperature (70°C), and produced high molecular weight polymer with unimodal molecular weight distributions, indicating the polymerization took place in a single-site nature. Complexes **3c–f** displayed better thermal stability than the corresponding complexes **2a–g** under similar conditions. In addition, copolymerizations of ethylene and 1-hexene with precatalysts **2a–g** were also explored in the presence of Et_2AlCl. Catalytic activity, comonomer incorporation, and properties of the resultant polymers can be controlled over a wide range by tuning catalyst structures and reaction parameters.© 2012 Wiley Periodicals, Inc. J Polym Sci Part A: Polym Chem 000: 000–000, 2012

KEYWORDS: catalysts; phenoxy-phosphine ligand; polyolefins; Ziegler-Natta polymerization

INTRODUCTION A significant number of advances in olefin polymerization catalysis have been reported in the past decade, and the development of new generation "nonmetallocene" catalysts has attracted great interest recently.[1–5] Among the transition metals, vanadium catalysts exhibited promising characteristics, especially for the syntheses of high molecular weight polyethylene,[6–10] syndiotactic polypropylene,[11,12] and poly(ethylene-*co*-propylene) and poly(ethylene-*co*-propylene-*co*-diene) elastomers.[13–15] Nonetheless, the reports on vanadium catalysts are limited owing to low activity, which is ascribed to their deactivation during the polymerization, especially at high polymerization temperature, due to reduction of catalytically active vanadium species to low valent, less active, or inactive species. This problem could be overcome by reactivation of inactive vanadium(II) center to active vanadium(III) species by addition of $Cl_3CCOOEt$ or chlorinated hydrocarbons (namely "rejuvenators" or "promoters" in the literature), which has proven to be effective reagents for maintaining the higher (active) oxidation state of vanadium systems.[16] Designing and synthesizing ancillary ligands to stabilize active vanadium species is another powerful approach to keep vanadium in high-oxidation and subsequently prolong the catalyst lifetime.[17–36] For example, Lorber et al. found the amine bis(phenolate) ligand can stabilize vanadium complexes that exhibited high activity for ethylene polymerization.[17] Nomura obtained many different (arylimino) vanadium complexes containing aryloxo and alkoxo ligands, which possessed excellent efficiency toward olefin (co)polymerization.[18,19] Aryloxide-based vanadyl complexes, reported by Redshaw's group, exhibited excellent performance in olefin polymerization at an elevated temperature.[20] However, complexes with high thermal stability in olefin polymerizations were scarce.

In Group 4 metal complexes, the phenoxide donors tend to be matched with relatively hard first-row nitrogen and oxygen-based donors.[37–40] Bearing hard nitrogen and oxygen-based donors, salicylaldiminato ligands have been used in

Additional Supporting Information may be found in the online version of this article.

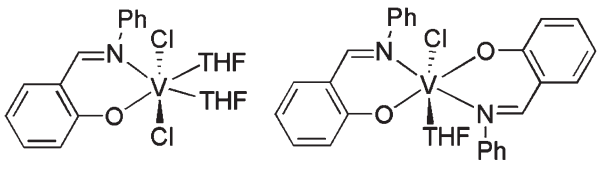

CHART 1 Previously reported salicylaldiminato vanadium-(iii) complexes.

transition metal organometallics and have already been shown to afford highly active olefin polymerization catalysts for Groups 4, 6,[41] and 10 metal systems.[42–44] Previously, our group had synthesized a series of mono and bis(salicylaldiminato) vanadium complexes, which showed high catalytic activity toward ethylene polymerization (Chart 1).[45,46] However, the deactivation or chain transfer to aluminum took place, and broad molecular weight distribution polymers were obtained at an elevated polymerization temperature by the mono salicylaldiminato vanadium(III) complexes. In addition, there is growing evidence that softer second-row donors may offer beneficial stabilization of the highly reactive metal center.[47–52] The combination of hard donors with soft phosphine donors in early transition metal polymerization catalysis increased the configurational stability of the catalyst, which was found by Gibson and Tang.[53–63] This work was initially aimed at introducing softer phosphine donors to the ligands, which were used to synthesize mono and bis(phenoxy-phosphine) vanadium complexes. These catalysts displayed some different characteristics from salicylaldiminato vanadium complexes for ethylene (co)polymerization.

EXPERIMENTAL

General Procedure and Materials

All manipulation of air- and/or moisture-sensitive compounds was carried out under a dry argon atmosphere using standard Schlenk techniques or under a dry argon atmosphere in an MBraun glovebox unless otherwise noted. All solvents were purified from an MBraun solvent purification system. The NMR data of the ligands were obtained on a Bruker 300 MHz spectrometer at an ambient temperature, with $CDCl_3$ as a solvent. The IR spectra were recorded on a Bio-Rad FTS-135 spectrophotometer. Elemental analyses were recorded on an elemental Vario EL spectrometer. Mass spectra were obtained using electron impact (EI-MS) and LDI-1700 (Linear Scientific). The NMR data of PE and ethylene/1-hexene copolymers were obtained on a Bruker 400 MHz spectrometer at 125°C with o-$C_6D_4Cl_2$ as a solvent. DSC measurements were performed on a Perkin–Elmer Pyris 1 differential scanning calorimeter at a rate of 10°C/min. The weight-average molecular weight (M_w) and the polydispersity index (PDI) of polymer samples were determined at 150°C by a PL-GPC 220 type high-temperature chromatograph equipped with three Plgel 10 μm Mixed-B LS type columns. 1,2,4-Trichlorobenzene (TCB) was employed as the solvent at a flow rate of 1.0 mL/min. The calibration was made by polystyrene standard EasiCal PS-1 (PL Ltd).

Ethyl trichloroacetate (ETA) were purchased from Aldrich, dried over calcium hydride at a room temperature, and then distilled. The *n*-butyllithium solution in hexane and $VCl_3(THF)_3$ was purchased from Aldrich. Et_2AlCl, $AlMe_3$, $AlEt_3$, and Al^iBu_3 were purchased from Albemarle Corporation. Modified methylaluminoxane (MMAO, 7% aluminum in heptane solution) was purchased from Akzo Nobel Chemical. Commercial ethylene was directly used for polymerization without further purification. The other reagents and solvents were commercially available. Various phenoxy-phosphine ligands containing different substituent on R_1 and R_2 positions, 2-R_1-4-R_2-6-PPh_2-C_6H_2OH (**2a**: R_1 = H, R_2 = H; **2b**: R_1 = F, R_2 = H; **2c**: R_1 = Ph, R_2 = H; **2d**: R_1 = *t*Bu, R_2 = H; **2e**: R_1 = Me, R_2 = Me; **2f**: R_1 = *t*Bu, R_2 = *t*Bu; **2g**: R_1 = CMe_2Ph, and R_2 = CMe_2Ph) were prepared according to literature procedures.[55,64,65]

Synthesis and Characterization of Vanadium Complexes

(2-PPh_2-C_6H_2O)$VCl_2(THF)_2$ (2a)

To a stirred solution of $VCl_3(THF)_3$ (0.75 g; 2.0 mmol) in dried tetrahydrofuran (THF) (20 mL) was added slowly a solution of 2-PPh_2-C_6H_2OH (0.56 g; 2.0 mmol) in THF (20 mL). The red reaction mixture was stirred for 10 min, and Et_3N (0.3 mL, 216 mg, and 2.1 mmol) was added. After stirring for 4 h at room temperature the solution was concentrated to about 10 mL, and then filtered to remove NH_4Cl. Crystallization by diffusion of *n*-hexane (20 mL) into the clear solution yielded red-black crystals of **2a** (0.65 g; 60%). Compounds **2b–g** were prepared analogously. IR (KBr pellets): *v* 3365, 3042, 2963, 1828, 1635, 1584, 1539, 1462, 1422, 1411, 1402, 1356, 1322, 1265, 1232, 1154, 1120, 1103, 1078, 1024, 976, 926, 872, 852, 757, 752, 728, 702, 658, 635, 563, 522, 493, and 434 cm^{-1}. EI-MS (70 eV): m/z = 542 [M^+]. Anal. Calcd for $C_{26}H_{30}ClO_3PV$: C, 57.47; H, 5.57. Found: C, 57.56; H, 5.51.

(2-F-6-PPh_2-C_6H_2O)$VCl_2(THF)_2$ (2b)

Yield: 69%. IR (KBr pellets): *v* 3414, 3059, 2967, 2953, 1971, 1903, 1822, 1601, 1575, 1553, 1466, 1441, 1382, 1310, 1262, 1237, 1193, 1123, 1068, 1027, 998, 896, 857, 780, 740, 727, 705, 693, 661, 618, 602, 561, 488, and 449 cm^{-1}. EI-MS (70 eV): m/z = 560 [M^+]. Anal. Calcd for $C_{26}H_{29}Cl_2FO_3PV$: C, 55.63; H, 5.21. Found: C, 55.46; H, 5.27.

(2-Ph-6-PPh_2-C_6H_2O)$VCl_2(THF)_2$ (2c)

Yield: 51%. IR (KBr pellets): *v* 3390, 3057, 2974, 2901, 1828, 1600, 1579, 1588, 1483, 1448, 1436, 1401, 1342, 1351, 1294, 1236, 1206, 1187, 1159, 1123, 1096, 1073, 1024, 999, 919, 875, 852. 803, 759, 752, 728, 702, 667, 635, 577, 563, 522, 491, and 467 cm^{-1}. EI-MS (70 eV): m/z = 618 [M^+]. Anal. Calcd for $C_{32}H_{34}Cl_2O_3PV$: C, 62.05; H, 5.53. Found: C, 62.11; H, 5.48.

(2-tBu-6-PPh_2-C_6H_2O)$VCl_2(THF)_2$ (2d)

Yield: 48%. IR (KBr pellets): *v* 3401, 3029, 2954, 2934, 1968, 1857, 1835, 1634, 1566, 1534, 1465, 1427, 1362,

1306, 1251, 1233, 1165, 1123, 1068, 1034, 992, 886, 868, 773, 740, 727, 705, 692, 654, 625, 602, 561, 476, and 455 cm^{-1}. EI-MS (70 eV): m/z = 598 [M^+]. Anal. Calcd for $C_{30}H_{38}Cl_2O_3PV$: C, 60.11; H, 6.39. Found: C, 60.15; H, 6.34.

(2-Me-4-Me-6-PPh$_2$-C$_6$H$_2$O)VCl$_2$(THF)$_2$ (2e)

Yield: 45%. IR (KBr pellets): ν 3254, 3015, 2876, 1815, 1633, 1576, 1526, 1438, 1421, 1401, 1378, 1356, 1324, 1263, 1232, 1151, 1119, 1087, 1032, 1024, 975, 958, 872, 864, 852, 773, 735, 716, 702, 648, 633, 620, 578, 534, 515, 476, and 422 cm^{-1}. EI-MS (70 eV): m/z = 570 [M^+]. Anal. Calcd for $C_{28}H_{34}Cl_2O_3PV$: C, 58.86; H, 6.00. Found: C, 58.75; H, 6.06.

(2-tBu-4-tBu-6-PPh$_2$-C$_6$H$_2$O)VCl$_2$(THF)$_2$ (2f)

Yield: 56%. IR (KBr pellets): ν 3321, 3017, 2952, 2923, 1965, 1832, 1807, 1634, 1563, 1525, 1467, 1423, 1361, 1325, 1278, 1233, 1165, 1123, 1068, 1034, 992, 886, 868, 763, 745, 737, 715, 682, 674, 621, 602, 563, 466, and 427 cm^{-1}. EI-MS (70 eV): m/z = 654 [M^+]. Anal. Calcd for $C_{34}H_{46}Cl_2O_3PV$: C, 62.29; H, 7.07. Found: C, 62.25; H, 7.01.

(2-CMe$_2$Ph-4-CMe$_2$Ph-6-PPh$_2$-C$_6$H$_2$O)VCl$_2$(THF)$_2$ (2g)

Yield: 53%. IR (KBr pellets): ν 3327, 3015, 2866, 1804, 1653, 1545, 1521, 1439, 1421, 1408, 1372, 1345, 1321, 1275, 1237, 1154, 1118, 1067, 1031, 1022, 977, 876, 865, 843, 772, 733, 725, 706, 639, 631, 575, 538, 520, 473, and 449 cm^{-1}. EI-MS (70 eV): m/z = 778 [M^+]. Anal. Calcd for $C_{34}H_{46}Cl_2O_3PV$: C, 67.78; H, 6.46. Found: C, 67.74; H, 6.42.

(2-Ph-6-PPh$_2$-C$_6$H$_2$O)$_2$VCl(THF) (3c)

To a stirred solution of $VCl_3(THF)_3$ (0.36 g; 1.0 mmol) in dried THF (20 mL) was added slowly a solution of 2-Ph-6-PPh_2-C_6H_2OH (0.71 g; 2.0 mmol) in THF (20 mL). The red reaction mixture was stirred for 20 min, and Et_3N (0.3 mL, 216 mg, and 2.1 mmol) was added. After stirring overnight at room temperature the solution was concentrated to about 10 mL and then the mixture was filtered to remove NH_4Cl. Crystallization by diffusion of *n*-hexane (20 mL) into the clear solution and chilling the solution (−40°C) yielded 0.535 g of **3c** (62%) as red-brown crystals. Compounds **3d–f** were prepared analogously. Yield: 51%. IR (KBr pellets): ν 3364, 3017, 2835, 1823, 1644, 1537, 1548, 1426, 1411, 1408, 1379, 1354, 1311, 1267, 1243, 1152, 1121, 1068, 1031, 1021, 973, 872, 861, 823, 771, 735, 716, 706, 633, 624, 572, 538, 523, 448, and 427 cm^{-1}. EI-MS (70 eV): m/z = 864 [M^+]. Anal. Calcd for $C_{52}H_{44}ClO_3P_2V$: C, 72.18; H, 5.13. Found: C, 72.11; H, 5.18.

(2-tBu-6-PPh$_2$-C$_6$H$_2$O)$_2$VCl(THF) (3d)

Yield: 51%. IR (KBr pellets): ν 3421, 3015, 2943, 2921, 1962, 1837, 1806, 1634, 1545, 1517, 1456, 1422, 1374, 1321, 1274, 1231, 1175, 1112, 1065, 1032, 998, 874, 856, 737, 711, 705, 647, 635, 621, 544, 466, and 438 cm^{-1}. EI-MS (70 eV): m/z = 824 [M^+]. Anal. Calcd for $C_{48}H_{52}ClO_3P_2V$: C, 69.86; H, 6.35. Found: C, 69.81; H, 6.28.

(2-Me-4-Me-6-PPh$_2$-C$_6$H$_2$O)$_2$VCl(THF) (3e)

Yield: 44%. IR (KBr pellets): ν 3321, 3016, 2942, 2927, 1953, 1832, 1807, 1632, 1544, 1512, 1453, 1427, 1371, 1321, 1269, 1231, 1174, 1132, 1078, 1037, 998, 874, 856, 823, 726, 717, 708, 663, 635, 628, 565, 447, and 433 cm^{-1}. EI-MS (70 eV): m/z = 768 [M^+]. Anal. Calcd for $C_{44}H_{44}ClO_3P_2V$: C, 68.71; H, 5.77. Found: C, 68.75; H, 5.69.

(2-tBu-4-tBu-6-PPh$_2$-C$_6$H$_2$O)$_2$VCl(THF) (3f)

Yield: 57%. IR (KBr pellets): ν 3411, 3021, 2866, 1862, 1641, 1537, 1548, 1426, 1411, 1408, 1379, 1354, 1311, 1267, 1225, 1143, 1108, 1066, 1031, 1021, 972, 866, 835, 812, 773, 724, 702, 664, 623, 572, 538, 448, and 427 cm^{-1}. EI-MS (70 eV): m/z = 936 [M^+]. Anal. Calcd for $C_{56}H_{68}ClO_3P_2V$: C, 71.75; H, 7.31. Found: C, 71.68; H, 7.25.

Ethylene Polymerization

Polymerization was carried out under atmospheric pressure in toluene in a 150 mL glass reactor equipped with a mechanical stirrer. Toluene (50 mL) was introduced into the nitrogen-purged reactor and stirred vigorously (600 rpm). The toluene was kept at a prescribed polymerization temperature, and then ethylene gas feed was started. After 15 min, a solution of Et_2AlCl in toluene and a solution of ETA in toluene were added and stirred for 5 min. Then a toluene solution of the vanadium complexes was added into the reactor with vigorous stirring (900 rpm) to initiate polymerization. After a prescribed time, acidic alcohol (10 mL) was added to terminate the polymerization reaction, and the ethylene gas feed was stopped. The resulting mixture was added to acidic alcohol. The solid polyethylene was isolated by filtration, washed with alcohol, and dried at 60°C for 24 h in a vacuum oven.

Ethylene/1-Hexene Copolymerization

Copolymerization was carried out in toluene in a 150 mL glass reactor equipped with a mechanical stirrer. The reactor was charged with 20 mL of toluene and the prescribed amount of 1-hexene. Next, the ethylene gas feed was started followed by equilibration at the desired polymerization temperature. After 15 min, a solution of Et_2AlCl in toluene and a solution of ETA in toluene were added and stirred for 5 min. Subsequently, a toluene solution of vanadium complexes was added into the reactor with vigorous stirring (900 rpm) to initiate polymerization. After a prescribed time, ethanol (10 mL) was added to terminate the polymerization reaction, and the ethylene gas feed was stopped. The resulting mixture was added to acidic ethanol. The polymer was isolated by filtration, washed with ethanol, and dried at 60°C for 12 h in a vacuum oven.

Crystallographic Studies

Crystals for X-ray analysis were obtained as described in the preparations. The crystallographic data, collection parameters, and refinement parameters are listed in Supporting Information Table S1. The crystals were manipulated in a glovebox. The intensity data were collected with the ω scan mode (186 K) on a Bruker Smart APEX diffractometer with CCD detector using Mo Kα radiation (λ = 0.71073Å). Lorentz, polarization factors were made for the intensity data, and absorption corrections were performed using the SADABS program. The crystal structures were solved using the SHELXTL program and refined using full matrix least squares. The positions of hydrogen atoms were calculated theoretically and included in the final cycles of refinement in a riding model along with attached carbons.

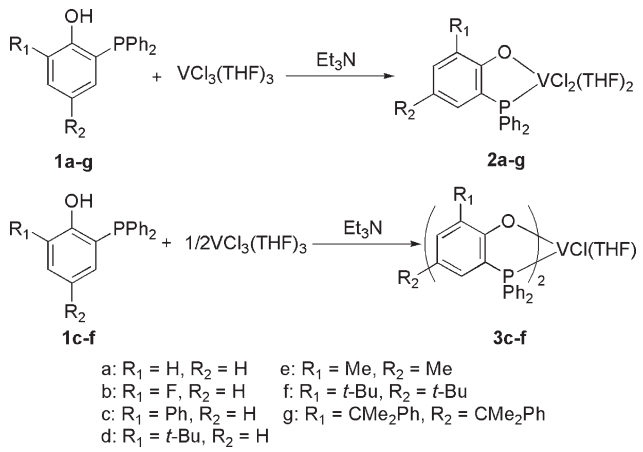

SCHEME 1 General synthetic route of the vanadium complexes used in this study.

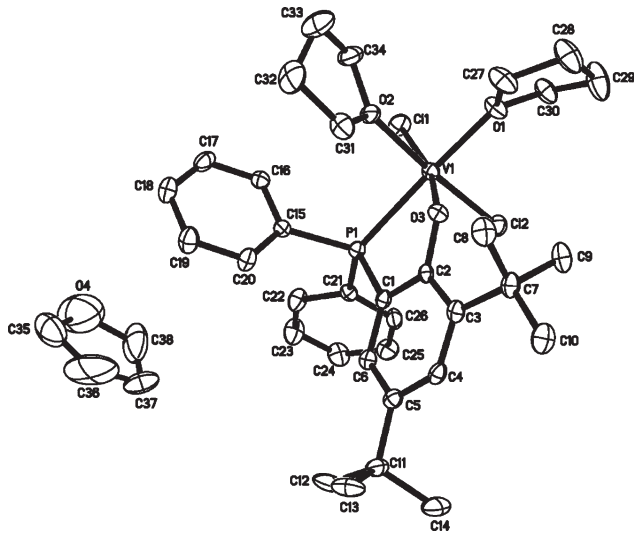

FIGURE 1 Molecular structure of complex 2f. Thermal ellipsoids are drawn at the 30% probability level, and H atoms are omitted for clarity.

RESULTS AND DISCUSSION

Synthesis and Characterization of Phenoxy-phosphine Vanadium(III) Complexes

A general synthetic route for new vanadium complexes used in this study is shown in Scheme 1. The phenoxy-phosphine ligands **1a–g** were prepared via the known procedure.[55,64,65] The reaction of $VCl_3(THF)_3$ with 1.0 equiv of 2-R_1-4-R_2-6-PPh_2-C_6H_2OH (**1a–g**) in THF in the presence of excess triethylamine (TEA) afforded vanadium(III) complexes **2a–g** in moderate yields (**2a**, 60%; **2b**, 69%; **2c**, 51%; **2d**, 48%; **2e**, 45%; **2f**, 56%; **2g**, 53%). These reactions took place along with evolution of hydrochloride, and the pure samples as dark red or brown crystallized solids were isolated from the chilled concentrated mixture of THF and hexane solution. These complexes were identified by FTIR and mass spectrum as well as elemental analyses (the sample was dried at room temperature for 5 h in a vacuum pump). The resonances are broadened to such an extent that they become effectively unobservable in the ^1H (or ^{13}C) NMR spectra for the complexes in $CDCl_3$ or C_6D_6, indicating that they are paramagnetic species.

Also shown in Scheme 1, reaction of $VCl_3(THF)_3$ with 2.0 equiv of phenoxy-phosphine ligands **1c-f** in the presence of excess TEA in THF afforded bis(phenoxy-phosphine) complexes **3c–f** in moderate yields (**3c**, 62%; **3d**, 51%; **3e**, 44%; **3f**, 57%). The reaction products were identified by mass spectra, FTIR, and elemental analysis. ^1H NMR spectra indicated that these complexes are also paramagnetic species, which is similar to the case of complexes **2a–g**.

The representative IR spectrums of **1c** and **2c** were studied and the results were present in Supporting Information Figure S1. It clearly indicated the disappearance of the band related to the O—H stretching in free ligand at about 3350 cm^{-1}. Instead, stretching frequencies of furan at about 3390, 3057, and 2974 cm^{-1} were observed. In addition, the strong band of ν(P-Ph) at around 1183 cm^{-1} shifts to lower frequency around 1123 cm^{-1}. The proposed structure is in line with the elemental analysis. Obvious difference in IR spectrums was observed for other ligands and the corresponding catalysts. However, IR spectra of mono and relevant bis(phenoxy-phosphine) vanadium were similar.

Crystals suitable for crystallographic analyses were grown from the chilled concentrated THF-hexane mixture solution. The ratio of THF-hexane was adjusted in the range of 1/1 to 1/3, according to the solubility of the complexes. A dark red block microcrystal of **2f** and **3c** suitable for X-ray crystallographic analysis was grown. The crystallographic data together with the collection and refinement parameters are summarized in Supporting Information Table S1. Molecular structures and the selected bond lengths and bond angles for **2f** and **3c** are shown in Figures 1 and 2.

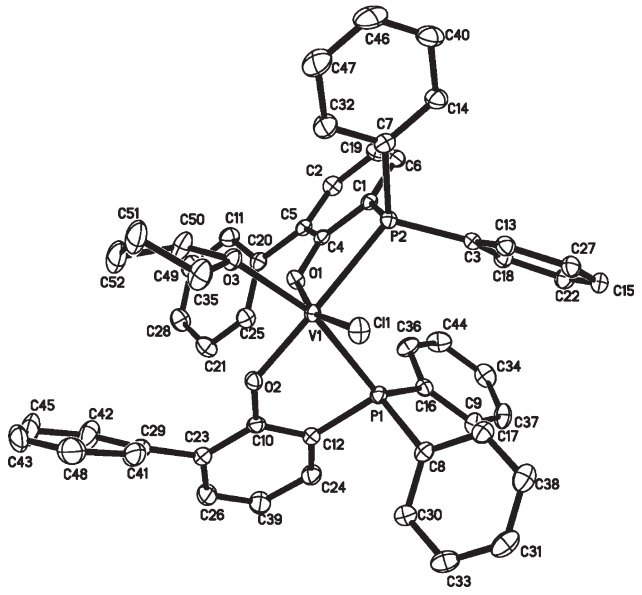

FIGURE 2 Molecular structure of complex 3c. Thermal ellipsoids are drawn at the 30% probability level, and H atoms are omitted for clarity.

As shown in Figure 1, complex **2f** has a six-coordinate distorted octahedral geometry around the V metal center. The two chlorine atoms are situated in the *cis* position, and the two THF molecules are also in *cis* position to each other, as seen in the bond angles for O(1)-V-O(2) (83.96°) and Cl(2)-V-Cl(3) (95.25°). However, in our previous work,[45] complex $[C_6H_5N{=}CH(OC_6H_2tBu_2\text{-}2,4)]\ VCl_2(THF)_2$, bearing the same substituents in the aryloxy group, possesses a different configuration, in which two chlorine atoms are situated in the *trans* position, while the two THF molecules are in *cis* position to each other. This may be due to steric hindrance of two benzene rings on the phosphorus atom.

Selected bond lengths (Å) and bond angles (deg): V-O(3), 1.897(4); V-O(1), 2.109(4); V-O(2), 2.162(4); V-Cl(2), 2.2968(17); V-Cl(1), 2.3345(17); V-P, 2.4943(17); O(3)-V-O(1), 92.20(15); O(3)-V-O(2), 83.69(15); O(1)-V-O(2), 83.96(15); O(3)-V-Cl(2), 95.11(12); O(1)-V-Cl(2), 91.69(12); O(2)-V-Cl(2), 175.43(12); O(3)-V-Cl(1), 166.17(13); O(1)-V-Cl(1), 96.63(12); O(2)-V-Cl(1), 86.67(11); Cl(2)-V-Cl(1), 95.25(6); O(3)-V-P, 78.33(11); O(1)-V-P, 170.41(12); O(2)-V-P, 93.37(11); Cl(2)-V-P, 90.70(6); Cl(1)-V-P, 92.40(6).

Compared with the structure of **II** and $[p\text{-}CF_3C_6H_4N{=}CH(C_6H_4O)]_2VCl(THF)$ reported previously,[52] complex **3c** displays different geometry, in which the equatorial positions are occupied by two phosphorus atoms of the phenoxy-phosphine ligand and two oxygen atoms, one from the THF molecule and the other from ligand (Fig. 2). Chlorine atom and oxygen atom from the ligand are coordinated on the axial position, which may also be attributed to the steric effect of diphenylphosphine substitute. The bond length V-P 2.5544Å in complex **3c** is slightly longer than **2f** (2.4943Å) and some reported vanadium complexes (2.367–2.500Å),[66,67] indicating that the interaction between V and P is not so strong, probably because two bulky coordinated ligands repulsed each other. The crowded environment of the two crystal structures may have a great influence on polymerization results. Other bond lengths, such as V-O, V-Cl in **2f** and **3c** are somewhat analogous.

Selected bond lengths (Å) and bond angles (deg): V-O(2), 1.8951(13); V-O(1), 1.9357(13); V-O(3), 2.1222(13); V-Cl(1), 2.3134(6); V-P(2), 2.5510(6); V-P(1), 2.5544(6); O(2)-V-O(1), 96.15(6); O(2)-V-O(3), 84.78(6); O(1)-V-O(3), 88.83(5); O(2)-V-Cl(1), 101.71(4); O(1)-V-Cl(1), 162.12(4); O(3)-V-Cl(1), 93.55(4); O(2)-V-P(2), 172.16(4); O(1)-V-P(2), 76.14(4); O(3)-V-P(2), 96.33(4); Cl(1)-V-P(2), 85.98(2); O(2)-V-P(1), 79.17(4); O(1)-V-P(1), 87.70(4); O(3)-V-P(1), 163.11(4); Cl(1)-V-P(1), 94.81(2); P(2)-V-P(1), 98.865(19).

Ethylene Polymerization

Co-catalysts, especially alkylaluminums, play an irreplaceable role in the olefin polymerization promoted by vanadium catalysts, and the performance of catalysts depended very much on the nature of the cocatalyst. In this article, we investigated the performance of complex catalyzing ethylene polymerization with the aid of various kinds of alkylaluminums, such as modified methylaluminoxane (MMAO), $AlMe_3$, $AlEt_3$, Al^iBu_3, and Et_2AlCl. $Cl_3CCOOEt$ (ETA) was used as a reactivating agent to reactivate the low-valent, less active, or inactive species to active vanadium(III) species. The typical results of the polymerization are collected in Table 1. The data in Table 1 (Entries 1–4 and 6) indicate that Et_2AlCl is the most effective cocatalyst among the five alkylaluminums under the similar conditions, while a much lower activity was obtained using MMAO or $AlMe_3$ or $AlEt_3$ as a cocatalyst, and even no polymer was formed using Al^iBu_3 as a cocatalyst, due to the strong reducibility. We found that $AlEt_2Cl$ displayed at least order of magnitude higher activities compared with (MMAO), $AlMe_3$, $AlEt_3$, and Al^iBu_3. Then we choose $AlEt_2Cl$ as cocatalyst for the following experiments. The catalytic activities of **2e** and **3e** first rapidly enhanced and then gradually declined with the increase of Al/V molar ratio, and the maximal value was obtained when the Al/V ratio equals 4000 (Fig. 3). However, the molecular weights of the polymer obtained gradually decreased with the increase of Et_2AlCl concentration, which indicates that chain transfer to aluminum took place during the polymerization. All the polymers prepared were linear polyethylene confirmed by ^{13}C NMR spectra, which is similar to that β-enaminoketonato or salicylaldiminato vanadium catalysts reported previously.[45,68]

The ^{13}C and ^{1}H NMR spectra revealed that the signals belonging to chain-end double bonds were not detected for low molecular weight copolymers, indicating that chain transfer to aluminum was the dominant chain-transfer pathway under these reaction conditions.

The reaction temperature considerably influenced polymerization behaviors, as shown in Figure 4. It is noteworthy that the catalytic activities of complexes **2a–g** displays the highest activities at 50°C, and then slightly decreased at 70°C. However, the molecular weights of the polymer obtained sharply decreased with the increase of reaction temperature, indicating that high temperature accelerates chain transfer reaction. In addition, substituents in the ligands greatly influence catalytic activities and the molecular weights of the polymers obtained. Complex **2a**, without any substituents on the ligand, displays relative low catalytic activity. Complex **2b**, bearing F-substituted phenoxy-phosphine ligand, also shows only low to mild catalytic activities, indicating that electron-withdrawing effects may be helpless for catalytic performance. Comparing **2c–g**, however, we found catalytic activities was improved from 13.4 (**2c**), 23.0 (**2d**) to 41.3 (**2f**) (kg PE/$mmol_V{\cdot}h{\cdot}bar$) with increasing of the steric hindrance, implying that introducing bulky substituents on aryloxy moiety of the phenoxy-phosphine ligand can efficiently improve catalytic activity. Although the steric hindrance of **2e**, bearing Me substituents, was not very large, it displayed higher activities (27.8) than **2c** and **2d**, indicating that para-methyl on aryloxy moiety of the phenoxy-phosphine ligand directly influences vanadium catalyst's performance. Complex **2g** bearing bulky CMe_2Ph on the aryloxy moiety, seeming to be an exceptant, exhibits relative low catalytic activity. Previous investigation showed that mono salicylaldiminato vanadium **I** produced the PE with broad molecular weight distributions when reaction temperature was 70°C, although it displayed

TABLE 1 Typical Results of Ethylene Polymerization by Complexes 2a–**g** and **3c–f**[a]

Entry	Complex	Temp (°C)	Cocatalyst	Time (min)	Polymer (g)	Activity[b]	M_w[c] ($\times 10^4$)	M_w/M_n[c]
1	**2f**	50	MMAO	10	0.03	0.36		
2	**2f**	50	Al^iBu_3	10	Trace	–		
3	**2f**	50	$AlEt_3$	10	0.01	0.12		
4	**2f**	50	$AlMe_3$	10	0.14	1.68		
5	**2f**	25	Et_2AlCl	5	1.48	35.5	12.3	2.4
6	**2f**	50	Et_2AlCl	5	1.72	41.3	4.2	2.1
7	**2f**	70	Et_2AlCl	5	1.23	29.5	2.3	3.1
8	**2a**	50	Et_2AlCl	5	0.27	6.48	6.3	2.4
9	**2b**	50	Et_2AlCl	5	0.31	7.44	5.7	1.9
10	**2c**	50	Et_2AlCl	5	0.56	13.4	5.2	2.4
11	**2d**	50	Et_2AlCl	5	0.96	23.0	4.2	3.0
12	**2e**	50	Et_2AlCl	5	1.16	27.8	6.1	2.7
13	**2g**	50	Et_2AlCl	5	0.58	13.9	5.7	1.8
14	**3c**	50	Et_2AlCl	5	0.64	15.4	6.8	2.7
15	**3d**	50	Et_2AlCl	5	0.59	14.2	5.5	2.2
16	**3e**	50	Et_2AlCl	5	0.63	15.1	8.2	2.6
17	**3f**	50	Et_2AlCl	5	0.94	22.6	7.6	2.0
18	**I**	25	Et_2AlCl	5	0.93	22.3	13.8	2.7
19	**I**	50	Et_2AlCl	5	0.88	21.1	5.7	3.8
20	**I**	70	Et_2AlCl	5	0.53	12.7	3.8	12.0
21	**II**	25	Et_2AlCl	5	0.35	8.4	17.1	1.9
22	**II**	50	Et_2AlCl	5	0.43	10.3	6.1	2.2
23	**II**	70	Et_2AlCl	5	0.41	9.84	1.5	2.6

[a] Reaction conditions: 1 bar of ethylene pressure, 0.5 μmol of vanadium complex, Cl_3CCO_2Et/V (molar ratio) = 300, Al/V (molar ratio) = 4000, toluene 50 mL.
[b] kg/mmol$_V$·h·bar.
[c] Determined by GPC in 1,2,4-trichlorobenzene versus polystyrene standard.

high catalytic activity. In contrast, **2d, 2e**, and **2f** not only showed much higher activities than **I**, but also produced polymers with relatively high molecular weights with unimodal molecular weight distributions, confirmed by GPC at 70°C, which attribute to benefits of introduction of softer second-row donor atoms and proper steric hindrance.

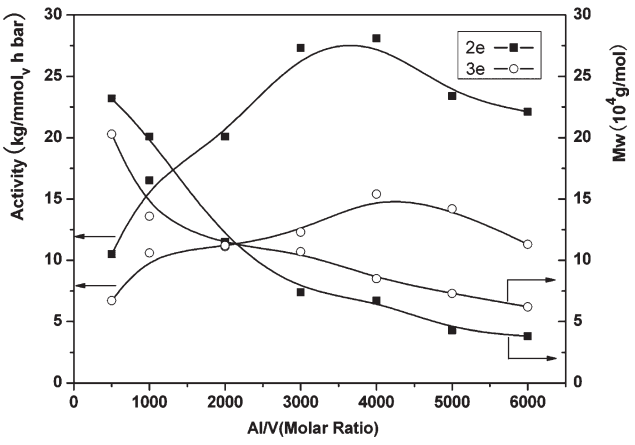

FIGURE 3 Plots of catalytic activity of vanadium complex and weight-average molecular weight of the polymers obtained vs. Al/V molar ratio. Reaction conditions: 0.5 μmol vanadium complex, Cl_3CCO_2Et 0.15 mmol, ethylene 1 atm, toluene 50 mL, and at 50°C polymerization for 5 min.

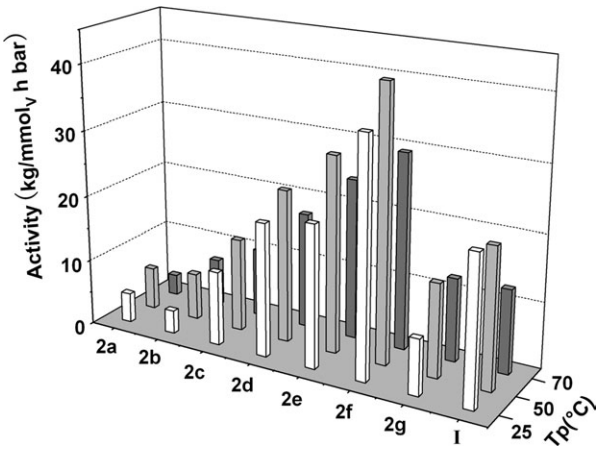

FIGURE 4 Catalytic activities of complexes 2a–g toward ethylene polymerization at different temperatures. Reaction conditions: 0.5 μmol of vanadium complex, Cl_3CCO_2Et 0.15 mmol, Et_2AlCl 2 mmol, ethylene 1 bar, toluene 50 mL, and polymerization for 5 min.

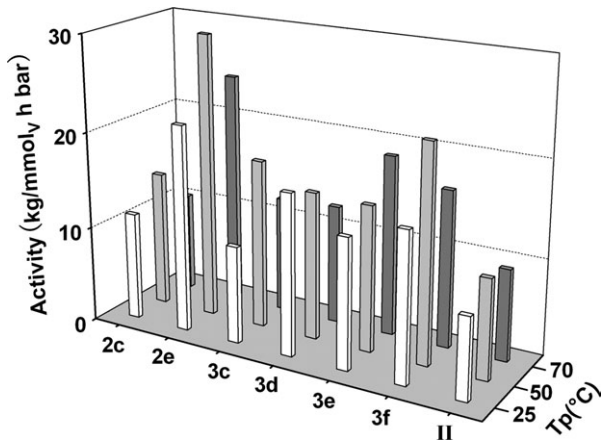

FIGURE 5 Catalytic activities of complexes 3c–f toward ethylene polymerization at different temperatures. Reaction conditions: 0.5 μmol of vanadium complex, Cl_3CCO_2Et 0.15 mmol, Et_2AlCl 2 mmol, ethylene 1 bar, toluene 50 mL, and polymerization for 5 min.

Although bis(salicylaldiminato) vanadium complexes are effective catalyst precursors for ethylene polymerization, they show much lower catalytic activities than mono salicylaldiminato complexes. In contrast, bis(phenoxy-phosphine) vanadium complexes **3c–f** show only slightly lower catalytic activities than monophenoxy-phosphine vanadium catalysts, as shown in Figure 5. Interestingly, all bis(phenoxy-phosphine) vanadium complexes displayed comparable activities under the same conditions. This is perhaps because the structures of bis(phenoxy-phosphine) vanadium complexes themselves already had the crowded environment, so that steric effect of the phenoxy moiety of the ligands was not so obvious as **2c–f**. An increase in reaction temperature from 50 to 70°C results in little decreasing catalytic activity for most of the complexes, while slightly enhancing catalytic activity for **3e**, suggesting the potential high thermal stability of these catalysts. This hypothesis could be confirmed in Supporting Information Figure S2. The catalytic activities of the phenoxy-phosphine complexes such as **2e** sharply decline with prolonged reaction time, while those of the bis(phenoxy-phosphine) complexes such as **3e** only slightly decrease. Moreover, all the bis(phenoxy-phosphine) vanadium complexes show much higher activities than **II** under the same condition, which may also attribute to benefits of introduction of softer second-row donor atoms.

Ethylene/Hexene Copolymerization by Complexes 2a–g

The copolymerizations of ethylene/1-hexene were also studied, and the representative results are summarized in Table 2. In the presence of cocatalyst Et_2AlCl and promoter $Cl_3CCOOEt$, catalysts **2a–g** show high activities towards ethylene/1-hexene copolymerization and produce copolymers with high molecular weight and unimodal molecular weight distributions. A quantitative ^{13}C NMR technique was used for measuring 1-hexene incorporation and microstructure of the copolymers. Chain termination mechanism in ethylene/hexene copolymerization coincides with ethylene polymerization, which observed from ^{13}C NMR spectra. The data of entries 1–6 and 14 in Table 2 indicate that catalytic activities was improved in the order of increasing steric bulk on aryloxy moiety of the phenoxy-phosphine ligand (**2a** < **2c** < **2d**, and **2e** < **2f**), implying that introducing bulky substituents can efficiently improve catalytic activity. However, continuing to increase steric bulk of the ligand, compared with catalyst **2f, 2g** display slightly lower activities for the copolymerization, which indicated that introduction of too bulky substituents was baleful to chain growth. Complex **2b**, bearing F-substituted phenoxy-phosphine ligand, also show only low to mild catalytic activities, indicating that electron-withdrawing effects may be harmful for catalytic performance. The data of entries 1–6 and 14 in Table 2 also indicated that the 1-hexene incorporation increases in the order of decreasing steric bulk on aryloxy moiety of the phenoxy-phosphine ligand (**2a/2b** > **2c** > **2d** and **2e** > **2f** > **2g**), which showed distinct regularity character.

The effect of reaction conditions on the copolymerization of ethylene/1-hexene was also investigated using catalyst **2f**. An enhancement in polymerization temperature from 25 to 50°C led to an increase in the catalytic activity (entry 6, 4.56 kg/mmol$_V$·h·bar; entry 7, 5.10 kg/mmol$_V$·h·bar) and 1-hexene incorporation (from 2.54% to 3.45%), but a decrease in the molecular weight of the resultant copolymer, while the molecular weight distribution of the copolymers almost remained constant. The increase of initial hexene concentration led to an increase in the 1-hexene incorporation (entries 6 and 8–11), while catalytic activity, the melting temperature, and the M_w of the resultant polymers gradually decreased. A dependence of catalytic activity on Et_2AlCl concentration is observed. As shown in entries 6, 12, and 13 (Table 2), a maximal activity of 4.56 kg/mmol$_V$·h·bar when the Al/V (molar ratio) equals 4000, whereas the molecular weight of the resultant polymers decreases with the increase of Al/V (molar ratio) from 1000 to 4000, indicating chain transfer reaction to Al occurred. Also the 1-hexene incorporation of the copolymer slightly increased with the increase of Et_2AlCl concentration. In addition, the molecular weight distributions remained constant, indicating a single-site catalytic behavior.

The microstructures of ethylene/1-hexene copolymers are established by ^{13}C NMR in o-$C_6D_4Cl_2$ at 125°C, with the assignment of the microstructure following previous work reported by Hsieh and Randall.[69,70] As shown in Figure 6, the resultant copolymer only possessed isolated 1-hexene inserted unit ([EHE] assigned as $T_{\delta\delta}$) among the repeated ethylene insertions when 1-hexene incorporation of the copolymer was not high (entries 6 and 9). However, when 1-hexene incorporation reached 11.4 mol% (entry 11), the resultant copolymer possessed isolated 1-hexene inserted unit ([EHE] assigned as $T_{\delta\delta}$) among the repeated ethylene insertions, and the alternating sequence ([HEH] assigned as $S_{\beta\beta}$) was also present with a low extent. In addition, the resonances ascribed to two 1-hexene repeating unit ([EHH] $T_{\beta\delta}$) were seen in the spectrum, and even tiny peaks due to block-type sequence of 1-hexene repeating units were

TABLE 2 Copolymerization of Ethylene and 1-Hexene by **2a–g**[a]

Entry	Complex	Temp. (°C)	1-Hexene (mol/L)	Polymer (g)	Activity[b]	Hexene Incorp[c]	M_w[d] ($\times 10^3$)	M_w/M_n[d]	T_m (°C)[e]
1	**2a**	25	0.2	0.14	0.84	3.75	41.1	2.2	105.3
2	**2b**	25	0.2	0.20	1.20	3.44	38.5	2.4	106.2
3	**2c**	25	0.2	0.33	1.98	3.11	47.2	2.6	109.3
4	**2d**	25	0.2	0.43	2.58	2.92	52.1	1.8	110.1
5	**2e**	25	0.2	0.39	2.34	2.96	49.4	2.1	110.5
6	**2f**	25	0.2	0.76	4.56	2.54	55.2	1.9	111.2
7	**2f**	50	0.2	0.85	5.10	3.45	28.2	1.7	106.3
8	**2f**	25	0.1	0.89	5.34	1.70	66.7	2.4	115.6
9	**2f**	25	0.4	0.53	3.18	5.68	35.4	2.6	101.3
10	**2f**	25	0.8	0.36	2.16	7.91	22.3	2.1	91.9
11	**2f**	25	1.2	0.25	1.50	11.4	12.4	2.5	78.2
12[f]	**2f**	25	0.2	0.53	3.18	2.66	80.2	2.3	110.3
13[g]	**2f**	25	0.2	0.68	4.08	2.60	61.3	2.0	110.5
14	**2g**	25	0.2	0.62	3.72	2.33	61.3	2.2	112.1

[a] Conditions: toluene + comonomer = 30 mL, ethylene 1 atm, catalyst 1.0 μmol, cocatalyst Et_2AlCl 4.0 mmol, ETA/V = 300 (molar ratio), 10 min.
[b] Activity in kg of polymer/mmol$_V$·h·bar.
[c] Comonomer content (mol %) estimated by ^{13}C NMR spectra.
[d] GPC data in 1,2,4-trichlorobenzene versus polystyrene standard.
[e] Determined by DSC.
[f] Al/V (molar ratio) = 1000.
[g] Al/V (molar ratio) = 2000.

observed (assigned as $S_{\alpha\alpha}$). The behavior is different from the resultant polymers obtained by the corresponding mono(β-enaminoketonato) vanadium(III) catalysts or $VCl_3(THF)_3$,[68] which only contained isolated hexene units even with high hexene incorporation (16.0 mol%). Moreover, as shown in Figure 6, the signals at 28.0 ppm ($S_{\beta\gamma}$), 32.5 ppm ($S_{\alpha\beta}$), and 38.9 ppm ($T_{\gamma\delta}$) caused by the inverse insertion sequences of 1-hexene were also found in the spectra. The possible monomer sequences in the copolymer were summarized in Scheme 2.

The triad distributions data and reactivity ratios r_e and r_h for each catalyst were calculated at 50°C according to ^{13}C NMR using the method of Hsieh and Randall, as shown in Table 3. The steric hindrance and electron effect of the

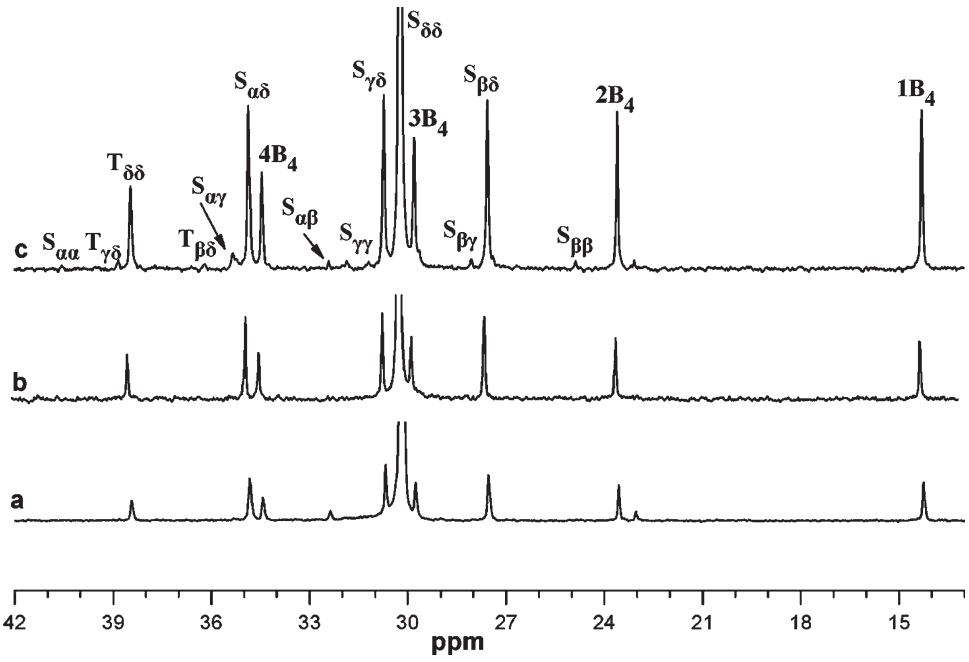

FIGURE 6 ^{13}C NMR of ethylene/1-hexene copolymer using catalyst 2f: (a) 2.54 mol % (entry 6); (b) 5.68 mol % (entry 9); (c) 11.4 mol % (entry 11) in Table 2.

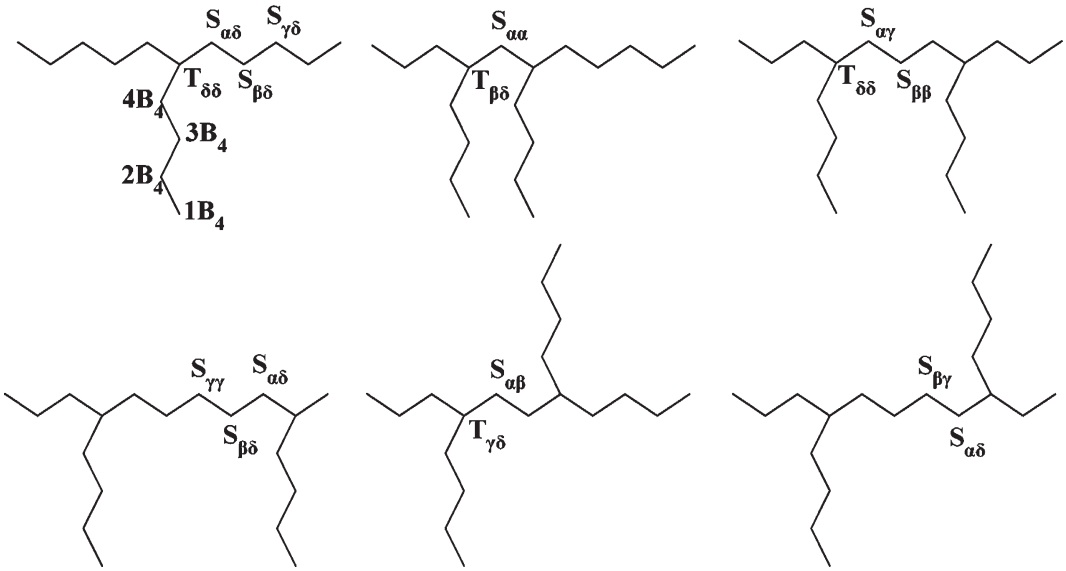

SCHEME 2 Possible monomer sequences in poly(ethylene-*co*-hexene)s.

ligands exerted obvious influence on the value of r_e and r_h, which manifested as the capability of incorporation of 1-hexene. Compared with complex **2a** ($r_h = 0.16$; $r_e = 31.4$), complex **2b** showed lower tendency to incorporate 1-hexene ($r_h = 0.08$; $r_e = 32.9$), indicating that electron-withdrawing effects may be unfavorable for 1-hexene insertion. The change in r_e from 31.4 (for **2a**) to 46.0 (for **2e**) is in turn more remarkable than r_h (from 0.01 to 0.17). We could also find that **2c** ($r_h = 0.17$; $r_e = 42.1$) showed a little higher tendency to incorporate 1-hexene than **2d** ($r_h = 0.14$; $r_e = 44.3$), which is broadly consistent with that at 25°C. Compared with complex **2e** ($r_h = 0.11$; $r_e = 46.0$), complex **2f** showed much lower tendency to incorporate 1-hexene ($r_h = 0.01$; $r_e = 45.9$), indicating that steric hindrance effect of the ligands may also be unfavorable for 1-hexene insertion. Finally, the value of 1-hexene incorporation of **2g** (0.030) is close to **2f** (0.031), which is a stark contrast with the results at 25°C, indicating that increasing temperature is beneficial for chain growth and 1-hexene insertion. These results indicate that the conclusions from reactivity ratios and 1-hexene incorporation calculated from ^{13}C NMR are unanimous. That is steric effect can hinder the insertion of 1-hexene, but high temperature can weaken this effect.

At last, we have tried to polymerize hexene alone. However, we have not found the white precipitation appearing, which maybe attributed to no polymer generation or getting a small amount of low molecular weight oligomer. For details, go to Supporting Information.

CONCLUSIONS

In summary, a series of vanadium(III) complexes bearing phenoxy-phosphine ligands have been synthesized, characterized and investigated as efficient catalysts for olefin polymerization. Both the ligand structures and the reaction parameters such as the cocatalyst type, the Al/V molar ratio and polymerization reaction temperature play an important role in ethylene polymerization. The steric hindrance effect can improve the catalytic performance of the mono phenoxy-phosphine vanadium complexes, and bis(phenoxy-phosphine) vanadium complexes exhibited higher thermal stability than mono complexes at high temperature due to the steric hindrance effect. The resultant polymers possessed high molecular weights with unimodal distributions, strongly suggesting that these polymerizations proceeded with a single catalytically active species. In addition, these complexes also exhibited high catalytic activity for ethylene/1-hexene

TABLE 3 Triad Distributions and Reactivity Ratios for Ethylene/1-Hexene Copolymerization

Cat.	$[H]_{feed}$	$[H]_{copolymer}$	[EHE]	[EHH]	[HHH]	[HEH]	[HEE]	[EEE]	r_e	r_h
2a	0.677	0.053	0.033	0.020	0.000	0.000	0.086	0.861	31.4	0.16
2b	0.677	0.046	0.037	0.010	0.000	0.000	0.083	0.870	32.9	0.08
2c	0.677	0.042	0.024	0.019	0.000	0.000	0.074	0.883	42.1	0.17
2d	0.677	0.038	0.025	0.013	0.000	0.000	0.063	0.899	44.3	0.14
2e	0.677	0.036	0.025	0.011	0.000	0.000	0.061	0.903	46.0	0.11
2f	0.677	0.031	0.030	0.009	0.000	0.000	0.061	0.900	45.9	0.01
2g	0.677	0.030	0.024	0.007	0.000	0.000	0.054	0.885	52.4	0.08

copolymerization. Changing the substituents in ligands significantly influenced the activity for ethylene polymerization and molecular weight of resultant polymers as well as the selectivity of 1-hexene. To further investigate the copolymerization system, the reactivity ratios of comonomers were determined using ^{13}C NMR methods of Hsieh and Randall. The steric hindrance and electronic effect of the ligands exert obvious influence on the value of r_e and $r_{h,}$ which manifested as the copolymerization capability of catalysts. We believe that the results through this study would introduce important information for designing efficient transition metal catalysts for olefin polymerization.

ACKNOWLEDGMENTS

The authors are grateful for subsidy provided by the National Natural Science Foundation of China (No. 20923003).

REFERENCES AND NOTES

1 Domski, G. J.; Rose, J. M.; Coates, G. W.; Bolig, A. D.; Brookhart, M. *Prog. Polym. Sci.* **2007,** *32*, 30–92.

2 Gibson, V. C.; Spitzmesser, S. K. *Chem. Rev.* **2003,** *103*, 283–315.

3 Britovsek, G. J. P.; Gibson, V. C.; Wass, D. F. *Angew. Chem. Int. Ed.* **1999,** *38*, 428–447.

4 Matsugi, T.; Fujita, T. *Chem. Soc. Rev.* **2008,** *37*, 1264–1277.

5 Stelzig, S. H.; Tamm, M.; Waymouth, R. M. *J. Polym. Sci. Part A: Polym. Chem.* **2009,** *47*, 6064–6070.

6 Natta, G.; Pasquon, I.; Zambelli, A. *J. Am. Chem. Soc.* **1962,** *84*, 1488–1490.

7 Carrick, W. L. *J. Am. Chem. Soc.* **1958,** *80*, 6455–6456.

8 Carrick, W. L.; Kluiber, R. W.; Bonner, E. F.; Wartman, L. H.; Rugg, F. M.; Smith, J. J. *J. Am. Chem. Soc.* **1960,** *82*, 3883–3887.

9 Lehr, M. H.; Carmen, C. *J. Macromolecules* **1969,** *2*, 217–219.

10 Lehr, M. H. *Macromolecules* **1968,** *1*, 178–184.

11 Zambelli, A.; Pasquon, I.; Signorini, R.; Natta, G. *Makromol. Chem.* **1968,** *112*, 160–182.

12 Doi, Y.; Kinoshita, J.; Morinaga, A.; Keii, T. *J. Polym. Sci. Polym. Chem. Ed.* **1975,** *13*, 2491–2497.

13 Christman, D. L.; Keim, G. I. *Macromolecules* **1968,** *1*, 358–363.

14 Doi, Y.; Suzuki, S.; Soga, K. *Macromolecules* **1986,** *19*, 2896–2900.

15 Addisson, E. *J. Polym. Sci. Part A: Polym. Chem.* **1994,** *32*, 1033–1041.

16 Christman, D. L. *J. Polym. Sci. Part A-1: Polym. Chem.* **1972,** *10*, 471–487.

17 Lorber, C.; Wolff, F.; Choukroun, R.; Vendier, L. *Eur. J. Inorg. Chem.* **2005,** 2850–2859.

18 Nomura, K.; Zhang S. *Chem. Rev.* **2011,** *111*, 2342–2362.

19 Nomura, K.; Zhang W. *J. Chem. Sci.* **2010,** *1*, 161–173.

20 Redshaw, C. *Dalton Trans.* **2010,** *39*, 5595–5604.

21 (a) Some other examples of vanadium catalysts see refs. 21–36; (b) Wu, J. Q.; Li, Y. S. *Coord. Chem. Rev.* **2011,** *255*, 2303–2314..

22 Wu, J. Q.; Li, Y. G.; Li, B. X.; Li, Y. S. *Chin. J. Polym. Sci.* **2011,** *29*, 627–633.

23 Chan, M.; Cole, J. M.; Gibson, V. C.; Howard, J. *Chem. Commun.* **1997,** 2345–2346.

24 Tomov, A. K.; Gibson, V. C.; Zaher, D.; Elsegood, M.; Dale, S. H. *Chem. Commun.* **2004,** 1956–1957.

25 Wu, J. Q.; Mu, J. S.; Zhang, S. W.; Li, Y. S. *J. Polym. Sci. Part. A: Polym. Chem.* **2010,** *48*, 1122–1132.

26 Cuomo, C.; Milione, S.; Grassi, A. *J. Polym. Sci. Part A: Polym. Chem.* **2006,** *44*, 3279–3289.

27 Milione, S.; Cavallo, G.; Tedesco, C.; Grassi, A. *Dalton Trans.* **2002,** *8*, 1839–1846.

28 Tang, L. M.; Wu, J. Q.; Duan, Y. Q.; Pan, L.; Li, Y. G.; Li, Y. S. *J. Polym. Sci. Part A: Polym. Chem.* **2008,** *46*, 2038–2048.

29 Hagen, H.; Bezemer, C.; Boersma, J.; Kooijman, H.; Lutz, M.; Spek, A. L.; van Koten, G. *Inorg. Chem.* **2000,** *39*, 3970–3977.

30 Janas, Z.; Wisniewska, D.; Jerzykiewicz, L. B.; Sobota, P.; Drabent, K.; Szczegot, K. *Dalton Trans.* **2007,** *20*, 2065–2069.

31 Bialek, M.; Czaja, K. *J. Polym. Sci. Part A: Polym. Chem.* **2008,** *46*, 6940–6949.

32 Bialek, M.; Liboska, O. *J. Polym. Sci. Part A: Polym. Chem.* **2010,** *48*, 471–478.

33 Nakayama, Y.; Bando, H.; Sonobe, Y.; Fujita, T. *J. Mol. Catal. A* **2004,** *213*, 141–150.

34 Zambelli, A.; Sessa, I.; Grisi, F.; Fusco, R.; Accomazzi, P. *Macromol. Rapid Commun.* **2001,** *22*, 297–310.

35 Bigmore, H. R.; Zuideveld, M. A.; Kowalczyk, R. M.; Cowley, A. R.; Kranenburg, M.; Mclnnes, E.; Mountford, P. *Inorg. Chem.* **2006,** *45*, 6411–6423.

36 Oakes, D. C. H.; Kimberley, B. S.; Gibson, V. C.; Jones, D. J.; White, A. J. P.; Williams, D. *J. Chem. Commun.* **2004, 2174–2182.**

37 (a) For recent reviews on bis(phenoxyimine) catalysts see refs. 48–51; (b) Mitani, M.; Saito, J.; Ishii, S.-I.; Nakayama, Y.; Makio, H.; Matsukawa, N.; Matsui, S.; Mohri, J.-I.; Furuyama, R.; Terao, H.; Bando, H.; Tanaka, H.; Fujita, T. *Chem. Rec.* **2004,** *4*, 137–158.

38 Nakayama, Y.; Bando, H.; Sonobe, Y.; Fujita, T. *Bull. Chem. Soc. Jpn.* **2004,** *77*, 617–625.

39 Makio, H.; Fujita, T. *Bull. Chem. Soc. Jpn.* **2005,** *78*, 52–66.

40 Sakuma, A.; Weiser, M.-S.; Fujita, T. *Polym. J.* **2007,** *39*, 193–207.

41 Jones, D. J.; Gibson, V. C.; Green, S. M.; Maddox, P. J.; White, A.; Williams, D. J. *J. Am. Chem. Soc.* **2005,** *127*, 11037–11046.

42 Wang, C. M.; Friedrich, S.; Younkin, T. R.; Li, R. T.; Grubbs, R. H.; Bansleben, D. A.; Day, M. W. *Organometallics* **1998,** *17*, 3149–3151.

43 Younkin, T. R.; Conner, E. F.; Henderson, J. I.; Friedrich, S. K.; Grubbs, R. H.; Bansleben, D. A. *Science* **2000,** *287*, 460–462.

44 Li, X. F.; Li, Y. S. *J. Polym. Sci. Part A: Polym. Chem.* **2002,** *40*, 2680–2685.

45 Wu, J. Q.; Pan, L.; Hu, N. H.; Li, Y. S. *Organometallics* **2008,** *27*, 3840–3848.

46 Wu, J. Q.; Pan, L.; Li, Y. G.; Liu, S. R.; Li, Y. S. *Organometallics* **2009,** *28*, 1817–1825.

47 Oakes, D. C. H.; Kimberley, B. S.; Gibson, V. C.; Jones, D. J.; White, A. J. P.; Williams, D. *J. Chem. Commun.* **2004, 2174–2175.**

48 Wang, C.; Ma, Z.; Sun, X. L.; Gao, Y.; Guo, Y.-H.; Tang, Y.; Shi, L. P. *Organometallics* **2006,** *25*, 3259–3266.

49 Froese, R. D. J.; Musaev, D. G.; Matsubara, T.; Morokuma, K. *J. Am. Chem. Soc.* **1997,** *119*, 7190–7196.

50 Froese, R. D. J.; Musaev, D. G.; Matsubara, T.; Morokuma, K. *Organometallics* **1999,** *18*, 373–379.

51 Porri, L.; Ripa, A.; Colombo, P.; Miano, E.; Capelli, S.; Meille, S. V. *J. Organomet. Chem.* **1996,** *514*, 213–217.

52 Lavanant, L.; Silvestru, A.; Faucheux, A.; Toupet, L.; Jordan, R. F.; Carpentier, J. F. *Organometallics* **2005,** *24*, 5604–5619.

53 Oakes, D. C. H.; Kimberley, B. S.; Gibson, V. C.; Jones, D. J.; White, A. J. P.; Williams, D. *J. Chem. Commun.* **2004,** 2174–2182.

54 Long, R. J.; Gibson, V. C.; White, A. J. P.; Williams, D. *J. Inorg. Chem.* **2006,** *45*, 511–513.

55 Long, R. J.; Gibson, V. C.; White, A. J. P. *Organometallics* **2008,** *27*, 235–245.

56 Hu, W. Q.; Sun, X. L.; Wang, C.; Gao, Y.; Tang, Y.; Shi, L. P.; Xia, W.; Sun, J.; Dai, H. L.; Li, X. Q.; Yao, X. L.; Wang X. R. *Organometallics* **2004,** *23*, 1684–1688.

57 Wang, C.; Sun, X. L.; Guo, Y. H.; Gao, Y.; Liu, B.; Ma, Z.; Xia, W.; Shi, L. P.; Tang, Y. *Macromol. Rapid Commun.,* **2005,** *26*, 1609–1614.

58 Wang, C.; Ma, Z.; Sun, X. L.; Gao, Y.; Guo, Y. H.; Tang, Y.; Shi, L. P. *Organometallics* **2006,** *25*, 3259–3266.

59 Gao, M.; Wang, C.; Sun, X.; Qian, C.; Ma, Z.; Bu, S.; Tang Y.; Xie, Z. *Macromol. Rapid Commun.* **2007,** *28*, 1511–1516.

60 Gao, M. L.; Gu, Y. F.; Wang, C.; Yao, X. L.; Sun, X. L.; Li, C. F.; Qian, C. T.; Liu, B.; Ma, Z.; Tang, Y.; Xie, Z.; Bu S. Z.; Gao Y. *J. Mol. Catal. A: Chem.* **2008,** *292*, 62–66.

61 Gao, M. L.; Tang, Y.; Xie, Z.; Bu S. Z.; Qian C. *J. Polym. Sci. Part A: Polym. Chem.* **2008,** *46*, 2807–2819.

62 Yang, X. H.; Sun, X. L.; Han, F. B.; Liu, B.; Tang, Y.; Wang, Z.; Gao, M. L.; Xie, Z.; Bu, S. Z. *Organometallics* **2008,** *27*, 4618–4624.

63 Yang, X. H.; Wang, Z.; Sun, X. L.; Tang, Y. *Dalton Trans.* **2009,** 8945–8954.

64 He, L. P.; Mu, H. L.; Li, B. X.; Li, Y. S. *J. Polym. Sci. Part A: Polym. Chem.* **2010,** *48*, 311–319.

65 He, L. P.; Liu, J. Y.; Li, Y. G.; Liu, S. R.; Li, Y. S. *Macromolecules* **2009,** *42*, 8566–8570.

66 Hsu, H. F.; Su, C. L.; Gopal, N. O.; Wu, C. C.; Chu, W. C.; Tsai, Y. F.; Chang, Y. H.; Liu, Y. H.; Kuo, T. S.; Ke, S. C. *Eur. J. Inorg. Chem.* **2006,** 1161–1167.

67 Chu, W. C.; Wu, C. C.; Hsu, H. F. *Inorg. Chem.* **2006,** *45*, 3164–3166.

68 Tang, L. M.; Wu, J. Q.; Duan, Y. Q.; Pan, L.; Li, Y. G.; Li, Y. S. *J. Polym. Sci. Part A: Polym. Chem.* **2008,** *46*, 2038–2048.

69 Reybuck, S. E.; Meyer, A.; Waymouth, R. M. *Macromolecules* **2002,** *35*, 637–643.

70 Hsieh, E. T.; Randall, J. C. *Macromolecules* **1982,** *15*, 1402–1406.